Virginia Commonwealth University

VCU Scholars Compass

Theses and Dissertations

Graduate School

2021

A COMPUTATIONAL MODEL RELATING TISSUE OXYGEN CONSUMPTION TO OXYGEN DELIVERY IN A KROGH CYLINDER MODEL OF SKELETAL MUSCLE

Raghad A. ALqahtani

Follow this and additional works at: https://scholarscompass.vcu.edu/etd

Part of the Other Physiology Commons, and the Systems and Integrative Physiology Commons

Downloaded from

https://scholarscompass.vcu.edu/etd/6749

A COMPUTATIONAL MODEL RELATING TISSUE OXYGEN CONSUMPTION TO OXYGEN DELIVERY IN A KROGH CYLINDER MODEL OF SKELETAL MUSCLE

A thesis submitted in partial fulfillment of the requirements for the degree of Master of Science at the Medical College of Virginia Campus, Virginia Commonwealth University.

Raghad Abdullah Alqahtani
Biomedical Engineering, Virginia Commonwealth University, 2019

Director:
ROLAND N. PITTMAN, Ph.D.
PROFESSOR
DEPARTMENT OF PHYSIOLOGY AND BIOPHYSICS

Virginia Commonwealth University
Richmond, Virginia
August 2021

Acknowledgment

The achievement of this work was only possible with some people's collaboration, encouragement, and support. I am sincerely grateful to those people who supported my success journey, motivated me, and guided me with enlightenment. During my study, I have been privileged to receive their encouragement and assistance. I want to acknowledge the following people for the critical role that I have played in this journey.

First and foremost, I thank my thesis mentor and director, Dr. Roland Pittman. Thank you for your patience, support, and appreciation through this process. Thank you for supporting me continually and urging me on this work. His positive attitude, guidance, motivating kept me concentrated on my goal. I could never have achieved this work without his knowledge and expertise. He worked very hard reviewing all my work and providing significant feedback promptly. When I felt stuck or tired or blocked, he was there to jumpstart my thought process. I would never made it to the end without his support.

I would also like to acknowledge and appreciate the committee members of my thesis project, Dr. Fadi Salloum and Dr. Martin Mangino, for their suggestions, meaningful feedback, and for their desire to serve as committee members. I appreciate you for spending your time and energy by serving on my committee. I thank you from the depths of my heart.

Writing this thesis and achieving the course work has been the most significant educational challenge of my career. I am grateful and fortunate to be supported by my wonderful parents, Abdullah and Ebtisam Alqahtani, and my siblings, Waad, Mutaeb, and Deem, who believe that I had the potential to do so much more with my career. My parents supported my journey and encouraged me to continue to strive for more. I know that their dream of me receiving a master was why I was able to get through this challenge. I dedicate this study to them with respect, love, and admiration. Then too, this thesis is dedicated to my fiancé, Mohammed. Thank you for your love, support, and abilities to cross an ocean to be with me, you made my journey pleasant in ways you will never know. Suffice me to say, "thanks," I am continually grateful to you.

Table of Contents

List of Tables

List of Figures

Abstract

A COMPUTATIONAL MODEL RELATING TISSUE OXYGEN CONSUMPTION TO OXYGEN DELIVERY IN A KROGH CYLINDER MODEL OF SKELETAL MUSCLE

By Raghad Abdullah Alqahtani, MS

A thesis submitted in partial fulfillment of the requirements for the degree of Master of Science at the Medical College of Virginia Campus, Virginia Commonwealth University.

Virginia Commonwealth University, 2021

Director:
Roland N. Pittman, Ph.D.
Department of Physiology and Biophysics

Oxygen transport from a capillary to skeletal muscle tissue is a complex process that involves convective and diffusive mechanisms to deliver adequate oxygen to meet tissue metabolic activities. Typically, oxygen uptake in tissue is set by oxygen demand, which is set by metabolic activity. The relationship between the oxygen consumption (VO_2) of an isolated perfused tissue and the rate of delivery of oxygen (QO_2) to the tissue has been a subject of interest to many investigators over the past century. Experiments have shown that there is a critical value of QO_2 below which tissue VO_2 begins to decline. The Michaelis-Menten kinetics model for oxygen-dependent oxygen consumption is investigated as a modeling assumption in a computational study of oxygen transport from capillaries to skeletal muscle tissue using the Krogh cylinder model. The work presented in this thesis extends Schumacker and Samsel's computational model to include the more accurate Michaelis-Menten kinetic description of the oxygen tension (PO_2) dependence of VO_2, using the parameter k_m, the PO_2 for half-maximal VO_2. This study aims to predict the relationship between oxygen consumption and oxygen delivery by considering the oxygen transport processes at the microvascular level. The dependence of oxygen consumption on oxygen delivery, critical oxygen extraction, critical oxygen delivery, and tissue oxygen tension profiles

were examined as a function of k_m. The critical oxygen delivery was found to depend on k_m, increasing nonlinearly as k_m increases. The fractional oxygen extraction at the critical QO_2 varied inversely with km. The venous oxygen partial pressure (PvO_2) also varied with k_m. Finally, the predicted radial profile of tissue oxygen tension at the critical QO_2 depended on k_m. At lower critical oxygen delivery and at lower k_m, the critical radial distance at which tissue oxygen partial pressure was found to be k_m occurred closer to the end of the capillary. The present results suggest that the value of k_m influences the relationship between tissue oxygen consumption and oxygen supply as the oxygen delivery is reduced to the critical point. Ultimately, k_m becomes the fundamental parameter that specifies how oxygen consumption depends on oxygen tension instead of the critical mitochondrial oxygen tension.

Introduction

The orchestrated work between the respiratory and cardiovascular systems helps to ensure the achievement of adequate energy production for cells by the metabolic action of mitochondria when the oxygen supply is adequate. The diffusion of oxygen from the alveoli to the pulmonary capillaries of the lung, oxygenates the blood, where it is pumped through the circulatory system by the heart (Costanzo, 1998). The oxygen in the red blood cells is carried by the protein hemoglobin, which is composed of four subunits, each with a heme group and a globin chain. Each of the four heme groups has an iron (Fe) atom in its center, which is the binding site for the oxygen carried in the blood to the body's organs (Pittman, 2016). Oxygen transport from capillary blood into the surrounding tissue occurs by passive diffusion that is driven by oxygen partial pressure gradients from the capillaries into the tissue. The oxygen is released from hemoglobin, where it diffuses from the red blood cell into the interstitial fluid, and moves across cell membranes and is then consumed by the mitochondria (Pishchany, 2012). The relationship between oxygen saturation (i.e., fraction of binding sites on hemoglobin occupied by oxygen) and oxygen partial pressure is described by the oxygen dissociation curve, where increases in oxygen partial pressure are related to increases in oxygen saturation or oxygen binding to hemoglobin. This curve is said to have a sigmoid shape, which illustrates the cooperative nature of oxygen binding to hemoglobin. Hemoglobin is highly saturated with oxygen in oxygen-rich blood, while reduction in blood oxygen partial pressure reduces the oxygen saturation, as oxygen is unloaded from red blood cells (Pittman, 2016). Within a cell, the oxygen partial pressure decreases as the mitochondria consume oxygen to produce energy, in the form of ATP, and thus, more oxygen diffuses from the interstitial fluid into the cell (Costanzo, 1998).

In skeletal muscle the transport of oxygen from the blood to the muscle tissue and finally to the mitochondria, where it is consumed, is a complex process, which involves convective and diffusive mechanisms to deliver adequate oxygen to meet tissue metabolic activities. The classical work of August Krogh from a century ago is usually assumed in many theoretical investigations of oxygen transport to tissues. Krogh's model made a number of simplifying assumptions: 1) in regard to oxygen transport, a tissue can be considered to be a collection of identical, parallel capillaries, each surrounded by a cylinder of homogeneous tissue; 2) one capillary supplies oxygen to the surrounding cylindrical tissue; 3) each capillary provides same amount of oxygen to the tissue; 4) oxygen tension within the capillary is uniform; 5) oxygen consumption is uniform in the tissue; 6) oxygen diffuses radially away from the capillary into the tissue; and 7) the flux of oxygen between tissue cylinders is zero thus eliminating the possibility of diffusive interactions between neighboring capillary/tissue cylinder units.

Normally, oxygen uptake in a tissue or the whole body is set by oxygen demand, which is in turn set by metabolic activity. Fick's principle can be applied to oxygen transport in the whole body, in an individual organ, or in a single microvessel (e.g., capillary) and the adjacent tissue it supplies. At the level of a Krogh tissue cylinder surrounding a single capillary, Fick's Principle states that "The amount of a substance consumed per unit time in a blood perfused tissue is equal to blood flow (Qc, flow in a single capillary) times the difference in arterial ([O2]a) and venous ([O2]v) concentrations of the substance," and can be stated succinctly in the following expression:

$$\dot{V}_{O_2} = \dot{Q}_c \, ([O_2]_a - [O_2]_v)$$

Multiplying and dividing the right-hand side of the equation by $[O_2]_a$

$$\dot{V}_{O_2} = \dot{Q}_c \, [O_2]_a \left(\frac{[O_2]_a - [O_2]_v}{[O_2]_a} \right)$$

Where the term $\dot{Q}_c\ [O_2]_a$ is the oxygen delivery in the capillary, which is the amount of oxygen delivered per unit time to the capillary, $(\frac{[O_2]_a-\ [O_2]_v}{[O_2]_a})$ is the oxygen extraction ratio, which is the fraction of oxygen removed from the arterial blood entering the capillary. Fick's principle defines the two components of oxygen transport: oxygen delivery, which represents the convective transport of oxygen determined by arterioles, and the oxygen extraction, which corresponds to the diffusion of oxygen to the tissue across the wall of the capillary. Under physiological conditions, oxygen exchange in the tissues is usually considered to be flow limited (Pittman, 2016). The oxygen delivery can be modified by blood flow determined by arteriolar tone, whereas the oxygen extraction can be modified by altering capillary density (related to intercapillary distance) or the surface area of the capillary. When the oxygen delivery is altered, oxygen consumption is maintained by reciprocal changes in oxygen extraction in an oxygen supply-independent phase. However, in the supply-dependent phase, oxygen uptake is found to decrease when the oxygen delivery decreases below the critical level (Schumacker & Samsel, 1989).

Previous experimental studies showed that the relationship between measured oxygen uptake at oxygen deliveries below the critical point has a linear relationship (Shibutani, 1983; Schumaker, 1987; Samsel, 1988; Eichacker, 1990). Schumacker's study suggested that in a Krogh cylinder model, oxygen supply limitation begins when the oxygen tension at the end of the capillary falls to point where oxygen diffusion from the capillary to the tissue cylinder surface is inadequate to maintain aerobic metabolism. Beyond the critical point of $PO_2 = 1$mmHg, which is too low to support tissue oxygen consumption and leads to a hypoxic region, occupying nearly 20% of the cylinder volume. Schumacker suggested that this linear relationship below the critical QO_2 point in stagnant hypoxia is due to a proportional decrease in the volume of aerobic tissue and therefore corresponds to a nearly linear decrease in overall tissue oxygen consumption

(Schumacker, 1989). In a previous study, Schumacker suggested that this linear relationship is a result of the tissue extraction that cannot increase below the critical delivery in proportion to the reduced delivery and oxygen consumption falls (Schumacker, 1987). However, other studies have shown that below the critical oxygen delivery, oxygen extraction can increase further (Cain, 1983), while another study reported that the oxygen extraction ratio at that threshold is the maximum (Cain, 1983).

Observations of heavily working human muscles have shown a venous blood oxygen saturation in the range of 15–30%, showing that extraction of oxygen is incomplete as a result of limited oxygen diffusion (Andersen, 1985; Rowell, 1986; Richardson, 1993; Richardson, 1995). Complete oxygen extraction would result in lower value of oxygen tension in the venous blood, which would not be high enough to support robust oxygen diffusion. In tissue with high oxygen demand, such as maximally working skeletal muscle, the maximum distance that oxygen can diffuse to the tissue from the capillary decreases with increasing oxygen uptake to match the oxygen demand of that tissue. A limitation of oxygen demand is the maximum rate of turnover of enzymes in the Krebs cycle that may limit the oxygen consumption in maximally working skeletal muscle. Blomstrand's study suggested that, of the Krebs cycle enzymes only oxoglutarate dehydrogenase showed a maximum activity and full activation during one-legged knee extension exercise, and thus, showed a correlation between oxoglutarate dehydrogenase and maximum oxygen consumption (Blomstrand, 1997). Additionally, oxygen diffusion to the mitochondria is one of the factors limiting the maximum oxygen consumption. Therefore, these limitation factors may all play a part in determining the maximum oxygen uptake.

Other studies have shown that oxygen uptake is dependent on blood flow. Bulkley showed that oxygen consumption is independent of blood flow until the flow is below 30 ml/min/100 g, at

which point the oxygen uptake by canine small intestine showed a marked flow-dependence (Bulkey, 1985). Similarly, Hughson's study on the onset of forearm exercise was influenced by muscle blood flow, which was tested with the arm either above or below heart level to modify perfusion pressure. Data that were obtained from different exercise intensities resulting in either minimal or moderate elevations of venous blood lactate, supported his hypothesis that oxygen consumption can be limited by the availability of oxygen. He has established that there is a significant positive correlation and a strong dependency of oxygen consumption on blood flow in forearm muscle (Hughson, 1996). More recent findings by Kalliokoski indicated that there is a good correlation between blood flow and oxygen consumption in different muscles during exercise, and that endurance-trained men might have a stronger correlation than untrained men. The data on blood flow and oxygen consumption in quadriceps femoris muscle in both trained and untrained individuals supported Kalliokoski's hypothesis (Kalliokoski, 2004).

Of the cellular respiration that occurs in mitochondria, more than 95% of the oxygen is consumed to produce energy (i.e., ATP) regardless of the oxygen concentration, unless the oxygen tension falls below 1 mmHg (Wilson, 1985). Under physiological conditions, this suggests that oxygen consumption is independent of oxygen partial pressure until almost all the oxygen at the location in question is used up. Many in vitro studies measured oxygen consumption rates in mitochondrial suspensions and showed cellular respiration would be maintained at either relatively low or high oxygen concentrations as long as the oxygen partial pressure was above the critical level of 1 mmHg. (Wilson, 1988). In a recent vivo study, Gloub and Pittman (2012) developed an approach to study the oxygen dependence of respiration in a skeletal muscle in situ, using oxygen partial pressure measurements in interstitial fluid made with phosphorescence quenching microscopy and rapid pneumatic compression of the tissue. The study suggested that the

mitochondria do not function in an on/off or all-or-nothing manner, but rather in a more graded manner over the entire range of physiological oxygen partial pressure (Golub & Pittman, 2012). A good representation of the oxygen dependency of mitochondrial respiration is assumed to be a "pseudo" Michaelis-Menten kinetics, which allows the maximal rate of consumption to be V^{max}, and the half-maximal rate to occur at $PO_2 = k_m$. In Wilson's study, this PO_2 dependence of oxygen consumption suggested that k_m would be well below 1 mmHg, while in Golub & Pittman study, k_m in the rat spinotrapezius muscle was approximately 10.5 mmHg. Based on these experiments and analysis, the rate of oxygen consumption appears to vary over a much wider range of physiological oxygen partial pressure levels than previously thought.

The aim of this project was to use a computational model for oxygen transport from a capillary to the tissue in a Krogh cylinder to study and predict the dependence of oxygen consumption on oxygen delivery for a range of k_m. A wide range of oxygen delivery is considered under conditions of high oxygen demand in which a significant fraction of the tissue volume becomes hypoxic, specifically, in stagnant hypoxia. The mathematical quantification of tissue oxygen delivery and consumption was based on systemic parameters, like cardiac output, blood oxygen partial pressure, arterial oxygen saturation, blood oxygen concentration, and venous oxygen partial pressure. As in the Krogh cylinder model, the capillaries are assumed to be parallel, unbranched, and each capillary supplies oxygen to a surrounding uniform cylindrical tissue. In previous in vivo studies, it was demonstrated that the dependency of oxygen consumption of skeletal muscle cells was on oxygen tension over a wider physiological range than previously proposed (Golub, Pittman, 2012). Oxygen consumption is assumed to depend on oxygen partial pressure according to Michaelis-Menten kinetics, where a range of k_m values were used, and the results are compared with those of Schumacker & Samsel (1989) and other previous studies.

Materials and Methods

The Assumptions of the Model

A mathematical model of oxygen tension distribution in a tissue cylinder was modeled using the assumptions proposed by August Krogh (Krogh, 1919). Krogh's cylinder model describes the oxygen transport in a microvascular unit consisting of a single capillary that supplies oxygen to a cylindrical tissue surrounding it. The prediction of Krogh's model, with several additional assumptions, was obtained with the assistance of his colleague, the mathematician Mr. K. Erlang. The assumptions may be set as the following:

- The capillary is uniform in dimensions, straight, and along the axis of each tissue cylinder.

- All capillaries are parallel, unbranched, and equally spaced.

- Tissues are identical, independent, parallel cylinders.

- The diffusive oxygen flow from the capillary is axially symmetric.

- At the surface of the capillary, the oxygen tension is constant, and the oxygen demand is uniform along the capillary length.

- The oxygen tension of the tissue at the capillary wall equals average oxygen tension inside the capillary.

- The oxygen consumption of the tissue is constant and uniform.

- The transfer of oxygen to the tissue is by diffusion only, and the diffusion constant is the same throughout the tissue.

- All microvascular oxygen transport phenomena are steady-state.

- Blood is a homogeneous fluid moving by plug flow and with complete radial mixing.

- Axial or longitudinal diffusion of oxygen in the tissue is not significant.

Selection of parameters. (Schumacker & Samsel)

The dimensions of the capillary were assumed to be a radius of 5 μm and a length of 500 μm. The tissue radius was one-half of the intercapillary distance of 80 μm. The estimated total blood volume was 500 ml, which corresponds to 1.27×10^{10} capillaries in a whole dog's body. The resting oxygen consumption was assumed to be 5×10^{-3} ml O2/min/g tissue. The oxygen diffusion coefficient in tissue was reported by Krogh as 2.1×10^{-8} cm^2 min^{-1} mmHg^{-1}. The cardiac output was 5000 ml/min, the hemoglobin concentration was 15 g/dl and the oxygen binding capacity was 1.34 mlO$_2$/gHb (Fig. 1). A summary of all parameters that were used are shown in Table. 1.

Capillary length (L)	500 μm
Capillary radius (r_c)	5 μm
Tissue length (L)	500 μm
Tissue radius (R)	40 μm
oxygen consumption ($\dot{V}_{O2}$)	5×10^{-3} ml/min/g
diffusion coefficient (D_{O2})	2.1×10^{-8} cm^2 min^{-1} mmHg^{-1}
hemoglobin concentration (Hb)	15 g/dl
oxygen binding capacity (C_{Hb})	1.34 mlO$_2$/g Hb
Cardiac output (CO)	5000 ml/min
Total number of capillaries	1.27×10^{10}
Blood flow (Q_c)	3.9370×10^{-7} ml/min

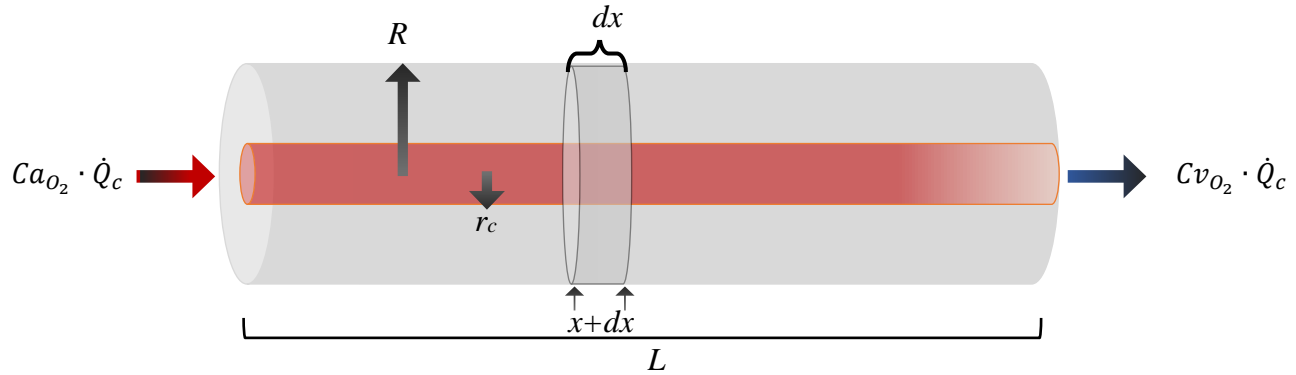*Table.1 Parameter values assumed for the capillary and tissues cylinder.*

Figure. 1. Schematic of Krogh tissue model, that shows the tissue cylinder radius $R=$ 40 μm (half of intercapillary distance of 80 μm), capillary radius $r_c=$ 5 μm, the total length of the capillary and tissue cylinder L= 500 μm, the differential disc thickness $dx=$ 5 μm, which was used in numerical integration of 100 steps along the capillary, the oxygen content at the arterial and venous ends of the capillary Ca_{O_2} and Cv_{O_2}, respectively, and the blood flow $\dot{Q}_c=$ 5×10^{-3} ml/min.

I. Schumacker model

i. Model of the Oxygen Tension, Oxygen Saturation, and Oxygen Content

The tissue cylinder and the capillary were partitioned longitudinally into equally spaced differential discs of 100 steps, so that each disc had a thickness of $dx = 5$ μm. The oxygen tension of the tissue then was computed with initial blood oxygen tension of 100 mmHg. Using the Krogh-Erlang equation, the oxygen tension at tissue surface as a function of radial distance from the capillary center was computed as the following:

$$P_{O_2 Surface} = P_{O_2 capillary}(x) - \frac{\dot{V}_{O_2}}{D_{O_2}} \cdot [\frac{R^2}{2} \cdot \ln\left(\frac{r}{r_c}\right) - \frac{(r^2 - r_c^2)}{4}] \quad \text{(Eq. 1)}$$

Where the $P_{O_{2_{capillary}}}(x)$ is the blood oxygen tension at the location x along the capillary, $\dot{V}_{O_2}$ is the rate of oxygen consumption per unit of tissue volume, D_{O_2} is Krogh's diffusion coefficient, R is the tissue radius, r_c is the capillary radius, r is the radial distance from the axis of the capillary to an arbitrary radial position in the tissue.

The oxygen saturation was computed for the blood in each disc by an equation (digital computer subroutine) that was proposed by Kelman (Kelman, 1966), which converts the oxygen tension to a saturation (i.e., the O2 dissociation curve).

$$S_{O_2} = 100 \cdot \frac{(a_1 x + a_2 x^2 + a_3 x^3 + x^4)}{(a_4 + a_5 x + a_6 x^2 + a_7 x^3 + x^4)} \qquad \text{(Eq. 2)}$$

Where x is the blood oxygen tension in the capillary; the values of the coefficients $a_1 \dots a_7$ are shown in Table. 2.

a_1	-8.5322289*10^3
a_2	2.1214010*10^3
a_3	-6.7073989*10^1
a_4	9.3596087*10^5
a_5	-3.1346258*10^4
a_6	2.3961674*10^3
a_7	-6.7104406*10^1

Table. 2 . The constant values of the coefficients $a_1 \dots a_7$, which were determined by curve-fitting technique in least-squares sense of oxygen tension and saturation (Kelman, 1996)

The steady-state mass balance equation was used to describe the gas exchange at any point x

along the capillary, and can be written for O_2 as:

$$\dot{Q}_{O_2}^{in} = \dot{Q}_{O_2}^{out} + \dot{V}_{O_2} \qquad \text{(Eq. 3)}$$

Which can be written as:

$$\dot{Q}_c \cdot C_{O_2}(x) = \dot{Q}_c \cdot C_{O_2}(x + dx) + \dot{V}_{O_2} \cdot A \cdot dx \qquad \text{(Eq. 4)}$$

Where $\dot{Q}_{O_2}^{in}$ is the oxygen delivery into the capillary, $\dot{Q}_{O_2}^{out}$ is the oxygen delivery out of the

capillary, $\dot{V}_{O_2}$ is the oxygen consumption, $\dot{Q}_c$ is the capillary blood flow, $C_{O_2}(x)$ and $C_{O_2}(x + dx)$

are the blood oxygen contents at the location x and the differential increment dx in the longitudinal

distance, and A is cross-sectional area of the oxygen-consuming tissue. The equation for the

change of oxygen content as a function of distance x can be derived by rearranging Eq. 4.

$$\frac{\partial C_{O_2}}{\partial x} = -\dot{V}_{O_2} \cdot A(x) \cdot \dot{Q}_c \qquad \text{(Eq. 5)}$$

$$C_{O_2}(x + dx) = C_{O_2}(x) - \dot{V}_{O_2} \cdot A \cdot (dx) \cdot \dot{Q}_c \qquad \text{(Eq. 6)}$$

$$\text{Where} \quad C_{O_2}(x) = Hb \cdot C_{Hb} \cdot S_{O_2}(x) \qquad \text{(Eq. 7)}$$

$$\text{and} \quad S_{O_2}(x + dx) = S_{O_2}(x) - \frac{\dot{V}_{O_2} \cdot A \cdot (dx)}{Hb \cdot C_{Hb} \cdot \dot{Q}_c} \qquad \text{(Eq. 8)}$$

ii. The method of solution

At the entry of the blood into the capillary, the oxygen tension was set at 100 mmHg and substituted in Eq. 1 to calculate the oxygen tension associated with the first disc at the surface of tissue. The oxygen saturation at the entry of the blood into the upstream face of the disc was calculated from Eq. 2, and oxygen content from Eq. 7. The corresponding values for the following disc were computed by calculating the oxygen content from the previous disc using Eq. 7 and substituting it into Eq. 6; then the oxygen saturation from the previous disc was calculated using Eq. 2 and substituting it into Eq. 8. Then, a linear interpolation was used in MATLAB to numerically solve for the local blood oxygen tension for the next disc. Finally, the new local blood oxygen tension was substituted into Eq. 1 to compute the oxygen tension of the new disc (Fig. 2). This procedure was repeated for the rest of the discs along the capillary and tissue.

$$\dot{V}_{O_2} \cdot A \cdot (dx)$$

$$S_{O_2}(x)$$
$$C_{O_2}(x)$$
$$P_{O_{2_{capillary}}}(x)$$
$$\dot{Q}_c$$
$$\dot{Q}_{O_2}^{in}$$

$$S_{O_2}(x+dx)$$
$$C_{O_2}(x+dx)$$
$$P_{O_{2_{Surface}}}$$
$$\dot{Q}_c$$
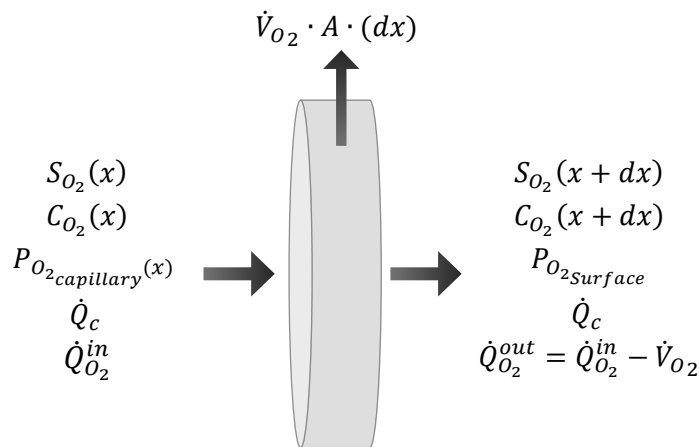$$\dot{Q}_{O_2}^{out} = \dot{Q}_{O_2}^{in} - \dot{V}_{O_2}$$

Figure. 2. Illustrates the relationship between variables in one disc of capillary and tissue cylinder.

iii. Oxygen delivery and uptake relationship

The relationship between oxygen delivery and uptake was then studied under conditions of stagnant hypoxia by decreasing oxygen delivery in stages and calculating the oxygen uptake. This was performed by lowering the cardiac output from 5000 ml/min in stages to about 5% of its initial value, while the oxygen content was maintained. The oxygen delivery was computed using the following formula:

$$\dot{Q}_{O_2} = Ca_{O_2} \cdot \dot{Q}_c \qquad \text{(Eq. 9)}$$

Where $\dot{Q}_{O_2}$ is the oxygen delivery, C_{O_2} is the oxygen content, and $\dot{Q}_c$ is the blood flow. In the Schumacker model, at each stage of lowered cardiac output, the oxygen consumption was computed depending on the cross-sectional area that was associated with the aerobic tissue, where $P_{O_{2_{Surface}}} > 1mmHg$, as a function of the distance along the capillary, and the $\dot{V}_{O_2}$ was considered normal. However, if the blood oxygen tension fell to the level where the $P_{O_{2_{Surface}}} < 1mmHg$, the cross-sectional area shrunk to include only the aerobic tissue at some distance r^* away from the capillary axis, and the oxygen consumption, $\dot{V}_{O_2}$, was calculated in the aerobic tissue at a radial distance of r_c -r^* ; however, there was no oxygen consumption in the anaerobic cross-sectional area of the tissue r^*-R . This radial distance, r^*, was computed using Eq. 1 by the Newton-Raphson method in MATLAB, where r^* was partitioned radially into equally spaced concentric rings of 100 steps that ranged from r_c -R (Fig. 3).
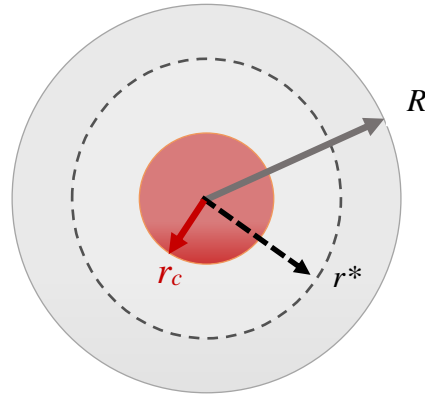
Figure. 3. Diagram illustrates the radial distance and variables in the cross-sectional area.

II.   *Michaelis-Menten model of oxygen consumption*

The Michaelis-Menten model was used to investigate oxygen tension dependence on oxygen consumption. Krogh's assumptions, equations (Eqs. 1-9) and the computational procedure of the Schumacker model was followed in computing blood and tissue oxygen tension, oxygen saturation, oxygen content and oxygen delivery. However, the oxygen consumption was assumed to depend on the oxygen tension according to Michaelis-Menten kinetics. Using the solution to the Krogh-Erlang equation for oxygen diffusion and consumption in the tissue

$$D_{O_2} \cdot \frac{1}{r} \cdot \frac{d}{dr} \cdot \left(r \cdot \frac{dP}{dr}\right) = V^{max} \qquad \text{(Eq. 10)}$$

Where D_{O_2} is the Krogh diffusion coefficient, P is the oxygen tension at a radial distance of r* within the tissue cylinder, and V^{max} is the maximum oxygen consumption rate per unit volume of the tissue cylinder. The boundary conditions for Eq. 10 are:

B.C. 1.   at r = r_c.   , $P_{O2} = P_c$

B.C. 2.   at r = R   , $\frac{dP}{dr} = 0$, since no oxygen flux at the tissue cylinder surface.

The tissue cylinder was divided into two radial regions to be considered for this model as the following:

Region I: $\quad r_c \leq r \leq r^*$ where $\quad k_m \leq P_{O2}$, $\quad \dot{V}_{O_2} = V^{max}$

Region II: $\quad r^* < r \leq R$ where $\quad P_{O2} < k_m$, $\quad \dot{V}_{O_2} = V^{max} \dfrac{P}{k_m}$

The equations for oxygen diffusion in the tissue cylinder for these two regions are:

Region I:

$$D_{O_2} \cdot \frac{1}{r} \cdot \frac{d}{dr} \cdot \left(r \cdot \frac{dP_I}{dr} \right) = V^{max} \qquad \text{(Eq. 11)}$$

$$\frac{d}{dr} \cdot \left(r \cdot \frac{dP_I}{dr} \right) = V^{max} \frac{r}{D_{O_2}}$$

Integration of both sides of the equation with respect to r:

$$P_I(r) = V^{max} \frac{r^2}{4 \cdot D_{O_2}} + C_1 \ln r + C_2 \qquad \text{(Eq. 12)}$$

Where $P_I(r)$ is the oxygen tension in region I at the radial distance of r_c to r^* within the tissue cylinder, D_{O_2} is the Krogh diffusion coefficient, V^{max} is the maximum oxygen consumption rate per unit volume of the tissue cylinder, and C_1 and C_2 are constants to be determined from the boundary conditions.

Region II:

$$D_{O_2} \cdot \frac{1}{r} \cdot \frac{d}{dr} \cdot \left(r \cdot \frac{dP_{II}}{dr} \right) = V^{max} \cdot \frac{P_{II}}{k_m} \qquad \text{(Eq. 13)}$$

Rearranging this equation to be in standard form:

$$D_{O_2} \cdot \frac{1}{r} \cdot \frac{d}{dr} \cdot \left(r \cdot \frac{dP_{II}}{dr} \right) - V^{max} \cdot \frac{P_{II}}{k_m} = 0 \qquad \text{(Eq. 14)}$$

$$\text{Where } b^2 = V^{max} \cdot \frac{P_{II}}{k_m}$$

The equation of the standard form is a second order differential equation using cylindrical coordinates and the solution to this equation yields Bessel functions.

$$P_{II}(r) = C_3 I_o(br) + C_4 K_o(br) \qquad \text{(Eq. 15)}$$

Where $P_{II}(r)$ is the oxygen tension in region II at the radial distance of r* to R within the tissue cylinder, I_o is a modified Bessel function of the first kind and zeroth order, K_o is a modified Bessel function of the second kind and zeroth order, C_3 and C_4 are constants.

There are four boundary conditions that are used to determine values of the four constants, which are

B.C. 1   at $r = r_c$, $P_I(r) = P_c$

B.C. 2   at $r = r^*$, $P_I(r^*) = P_{II}(r^*)$ Continuity of P_{O2} at the boundary.

B.C. 3   at $r = r^*$, $\left.\dfrac{dP_I}{dr}\right|_{r^*} = \left.\dfrac{dP_{II}}{dr}\right|_{r^*}$ Continuity of O_2 flux at the boundary.

B.C. 4   at $r = R$, $\left.\dfrac{dP_{II}}{dr}\right|_R = 0$ No O_2 flux at the surface of tissue cylinder.

Applying the boundary conditions, a set of the linear equations were obtained which were solved for the four constants, C_1 –C_4.

B.C. 1 $P_I(r) = V^{max}\dfrac{r_c^2}{4\cdot D_{O_2}} + C_1 \ln r_c + C_2 = P_c$

B.C. 2 $V^{max}\dfrac{r^{*2}}{4\cdot D_{O_2}} + C_1 \ln r^* + C_2 = C_3 I_o(br^*) + C_4 K_o(br^*)$

B.C. 3 $V^{max}\dfrac{r^*}{2\cdot D_{O_2}} + C_1 \dfrac{1}{r^*} = C_3 bI_1(br^*) - C_4 bK_1(br^*)$

B.C. 4 $0 = C_3 bI_1(bR) - C_4 bK_1(bR)$

The following expressions for the boundary conditions were used to solve for constants $C_1 - C_4$

B.C. 1 $\qquad C_1 \ln r_c + C_2 = P_c - V^{max} \dfrac{r_c^2}{4 \cdot D_{O_2}}$

B.C. 2 $\qquad C_1 \ln r^* + C_2 - C_3 I_0(br^*) - C_4 K_0(br^*) = -V^{max} \dfrac{r^{*2}}{4 \cdot D_{O_2}}$

B.C. 3 $\qquad C_1 \dfrac{1}{r^*} - C_3 \, bI_1(br^*) + C_4 bK_1(br^*) = -V^{max} \dfrac{r^*}{2 \cdot D_{O_2}}$

B.C. 4 $\qquad C_4 = \dfrac{I_1(b\mathrm{R})}{K_1(b\mathrm{R})} C_3$

Substitute B.C. 4 into B.C. 2 and B.C. 3 to get the linear equations for $C_1 - C_3$; the three equations

for these constants are:

$$C_1 \ln r_c + C_2 = P_c - V^{max} \dfrac{r_c^2}{4 \cdot D_{O_2}}$$

$$C_1 \ln r^* + C_2 - C_3 \left[I_0(br^*) + K_0(br^*) \cdot \dfrac{I_1(b\mathrm{R})}{K_1(b\mathrm{R})} \right] = -V^{max} \dfrac{r^{*2}}{4 \cdot D_{O_2}}$$

$$C_1 - C_3 \, br^* [I_1(br^*) - K_1(br^*) \cdot \dfrac{I_1(b\mathrm{R})}{K_1(b\mathrm{R})}] = -V^{max} \dfrac{r^{*2}}{2 \cdot D_{O_2}}$$

To simplify the equations, define:

$$A_2 = I_0(br^*) + K_0(br^*) \cdot \dfrac{I_1(b\mathrm{R})}{K_1(b\mathrm{R})}$$

$$A_3 = br^* [I_1(br^*) - K_1(br^*) \cdot \dfrac{I_1(b\mathrm{R})}{K_1(b\mathrm{R})}]$$

Rewrite the linear equations to get:

$$C_1 \ln r_c + C_2 = P_c - V^{max} \dfrac{r_c^2}{4 \cdot D_{O_2}}$$

$$C_1 \ln r^* + C_2 - A_2 C_3 = -V^{max} \dfrac{r^{*2}}{4 \cdot D_{O_2}}$$

$$C_1 - A_3 C_3 = -V^{max} \frac{r^{*2}}{2 \cdot D_{O_2}}$$

Solve for these three simultaneous linear equations for $C_1 - C_3$ using determinants:

$$D = \begin{bmatrix} \ln r_c & 1 & 0 \\ \ln r^* & 1 & -A_2 \\ 1 & 0 & -A_3 \end{bmatrix} = A_3 \ln\left(\frac{r^*}{r_c}\right) - A_2$$

Solve for $C_1 - C_3$. Note that D is the discriminant of the determinant and not Krogh's diffusion coefficient.

$$C1 = \begin{bmatrix} P_c - V^{max} \frac{r_c^2}{4 \cdot D_{O_2}} & 1 & 0 \\ -V^{max} \frac{r^{*2}}{4 \cdot D_{O_2}} & 1 & -A_2 \\ -V^{max} \frac{r^{*2}}{2 \cdot D_{O_2}} & 0 & -A_3 \end{bmatrix} \cdot D^{-1}$$

$$C1 = \frac{1}{D}\left[(-A_3)\left(P_c - V^{max}\frac{r_c^2}{4 \cdot D_{O_2}} + V^{max}\frac{r^{*2}}{4 \cdot D_{O_2}}\right) + (A_2 V^{max}\frac{r^{*2}}{2 \cdot D_{O_2}})\right].$$

$$C2 = \begin{bmatrix} \ln r_c & P_c - V^{max}\frac{r_c^2}{4 \cdot D_{O_2}} & 0 \\ \ln r^* & -V^{max}\frac{r^{*2}}{4 \cdot D_{O_2}} & -A_2 \\ 1 & -V^{max}\frac{r^{*2}}{2 \cdot D_{O_2}} & -A_3 \end{bmatrix} \cdot D^{-1}$$

$$C2 = \frac{1}{D}\left[-\left(P_c - V^{max}\frac{r_c^2}{4 \cdot D_{O_2}}\right)\left(-A_3 \ln\left(\frac{r^*}{r_c}\right) + A_2\right) - \left(V^{max}\frac{r^{*2}}{4 \cdot D_{O_2}}\right)(-A_3 \ln(r_c)) + \right.$$

$$\left. \left(V^{max}\frac{r^{*2}}{4 \cdot D_{O_2}}\right)(-A_2 \ln(r_c))\right].$$

$$C3 = \begin{bmatrix} \ln r_c & 1 & P_c - V^{max}\dfrac{r_c^2}{4 \cdot D_{O_2}} \\[2em] \ln r^* & 1 & -V^{max}\dfrac{r^{*2}}{4 \cdot D_{O_2}} \\[2em] 1 & 0 & -V^{max}\dfrac{r^{*2}}{2 \cdot D_{O_2}} \end{bmatrix} \cdot D^{-1}$$

$$C3 = \frac{1}{D}\left[-\left(P_c - V^{max}\frac{r_c^2}{4 \cdot D_{O_2}}\right) - \left(V^{max}\frac{r^{*2}}{4 \cdot D_{O_2}}\right) - \left(V^{max}\frac{r^{*2}}{4 \cdot D_{O_2}}\right)\left(\ln\left(\frac{r_c}{r^*}\right)\right)\right].$$

The resulting differential equation was nonlinear; however, an approximation was made for the Michaelis-Menten kinetic equation for oxygen consumption in the tissue cylinder as a piecewise linear expression with two regions: a P_{O2}-independent region at which $k_m < P_{O2}$ in Region I, and a P_{O2}-dependent region at $0 < P_{O2} < k_m$ in Region II.

The tissue oxygen consumption of region I, P_{O2}-independent, was associated with the cross section of the tissue cylinder, i.e.,

$$\dot{V}_{O_2} = V^{max}\,\pi\left(r^{*2} - r_c^2\right)dx \qquad \text{(Eq. 16)}$$

The oxygen consumption per unit length of region II, P_{O2}-dependent, was founded by numerically integrating the consumption per unit volume over the cross section of the tissue cylinder, i.e.,

$$\dot{V}_{O_2} = \frac{V^{max}}{k_m} \cdot 2\pi \cdot dx \int_{r^*}^{R} P_{II}(r)\, r\, dr \qquad \text{(Eq. 17)}$$

The total oxygen consumption for one disc was computed as:

$$\dot{V}_{O_2} = \dot{V}_{O_2}(I) + \dot{V}_{O_2}(II) \qquad \text{(Eq. 18)}$$

Where $\dot{V}_{O_2}(I)$ is the oxygen consumption for region I , and $\dot{V}_{O_2}(II)$ is the oxygen consumption for region II. This equation was computed for every disc along the capillary, where the oxygen consumption for region I, $\dot{V}_{O_2}(I)$, was computed from (Eq.16), and oxygen consumption for region

II, $\dot{V}_{O_2}(II)$, was computed from (Eq.17). The results were then plotted against the oxygen delivery

for each reduced cardiac output, and were then normalized (scaled) to the whole body (Fig 4-5).

Results:

The oxygen delivery and consumption model of Schumacker and Samsel (1989) was

repeated and numerically solved in MATLAB to compare it with the assumed Michaelis-Menten

oxygen consumption kinetics, and a graph was produced (Fig. 4). To assess the sensitivity of the

oxygen delivery and consumption to the assumed Michaelis-Menten oxygen consumption kinetics,

calculations using a range of values of k_m were carried out with the approximation that local oxygen

consumption was the maximum for PO_2 greater than k_m; then, for $PO_2 < k_m$, the oxygen

consumption is given by Eq. 17. Figure. 4 shows the comparison of the effect of the Schumacker

and Samsel model and the assumed Michaelis-Menten oxygen consumption kinetics on the

relationship between oxygen consumption and delivery during stagnant hypoxia by increasing the

values of k_m. Oxygen consumption remained constant and in a supply-independent phase in both

models until a critical oxygen delivery was reached. Below this critical oxygen delivery point, a

linear fall of oxygen consumption was associated with a reduction of oxygen delivery in a supply-

dependent phase in Schumacker and Samsel model. However, for Michaelis-Menten oxygen

consumption kinetics, increasing the value of k_m, led to a non-linear relationship between oxygen

consumption and oxygen delivery below the critical point of oxygen delivery. Figure. 5 shows the

oxygen delivery critical points for different values of $k_m = 10, 15,$ and 25 mmHg.
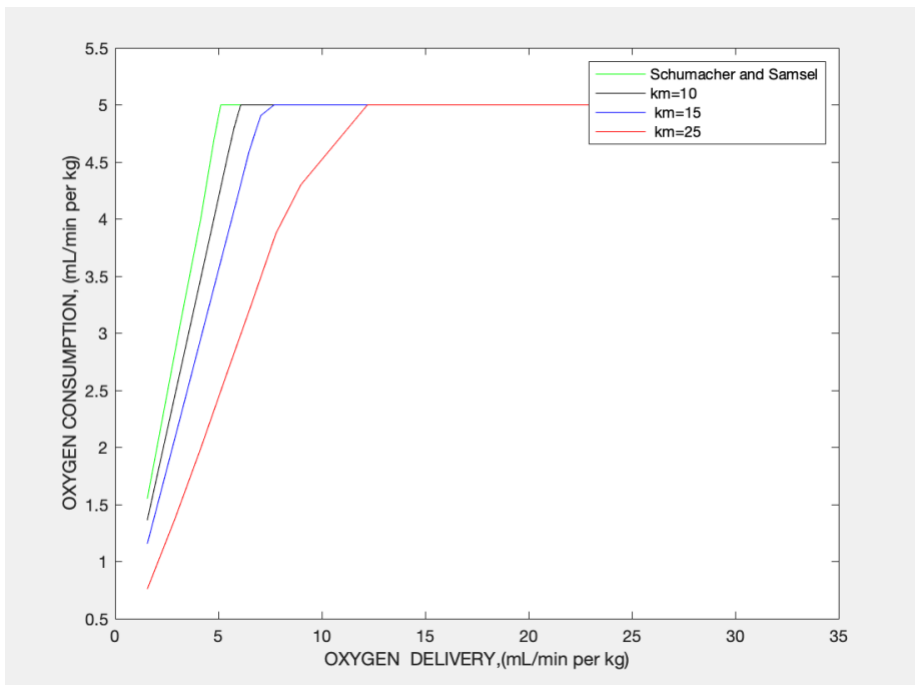
Figure. 4. Oxygen consumption and delivery. Variation of oxygen consumption and delivery showing the Schumacker and Samsel graph (green), and the effect of different k_m values on oxygen consumption and delivery.
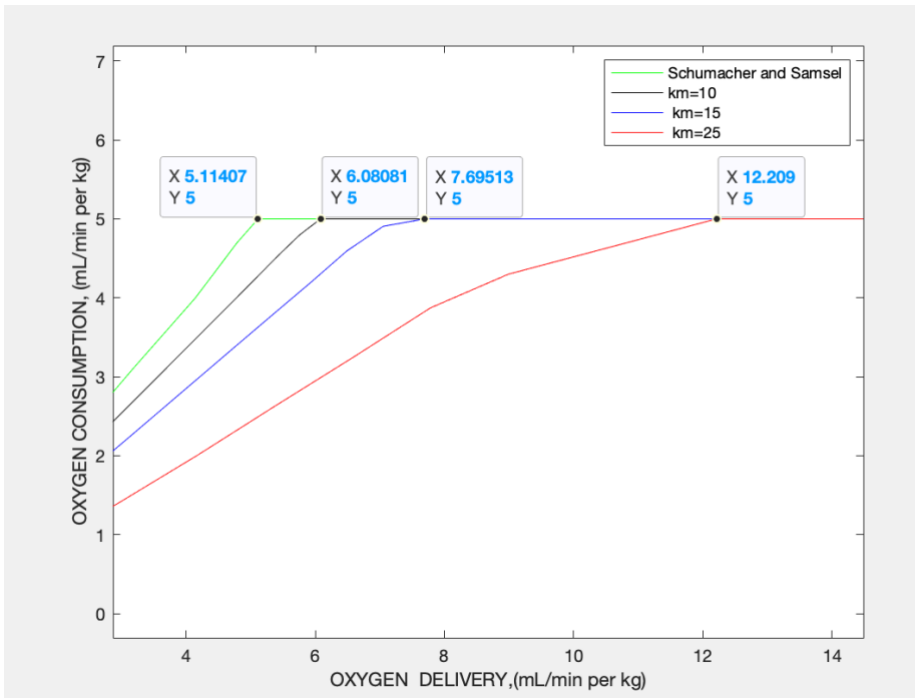

Figure. 5. Relationship between oxygen consumption and oxygen delivery. The critical values of oxygen delivery are shown for different values of k_m = 10, 15, and 25 mmHg.

A plot of the critical oxygen delivery versus k_m is shown in Figure. 6. The relationship between k_m and critical oxygen delivery is nonlinear, with the critical QO_2 increasing with k_m.

The oxygen extraction ratio is a way of describing the adequacy of systemic oxygen delivery. The oxygen extraction ratio at the critical oxygen delivery points was plotted against k_m values and shown in Figure. 7. They exhibit an inverse nonlinear relationship , whereby oxygen extraction, expressed as a percentage, decreases as k_m increases. In the capillary, when the oxygen delivery decreases, the oxygen extraction ratio increases as the tissue extracts more of the delivered oxygen.
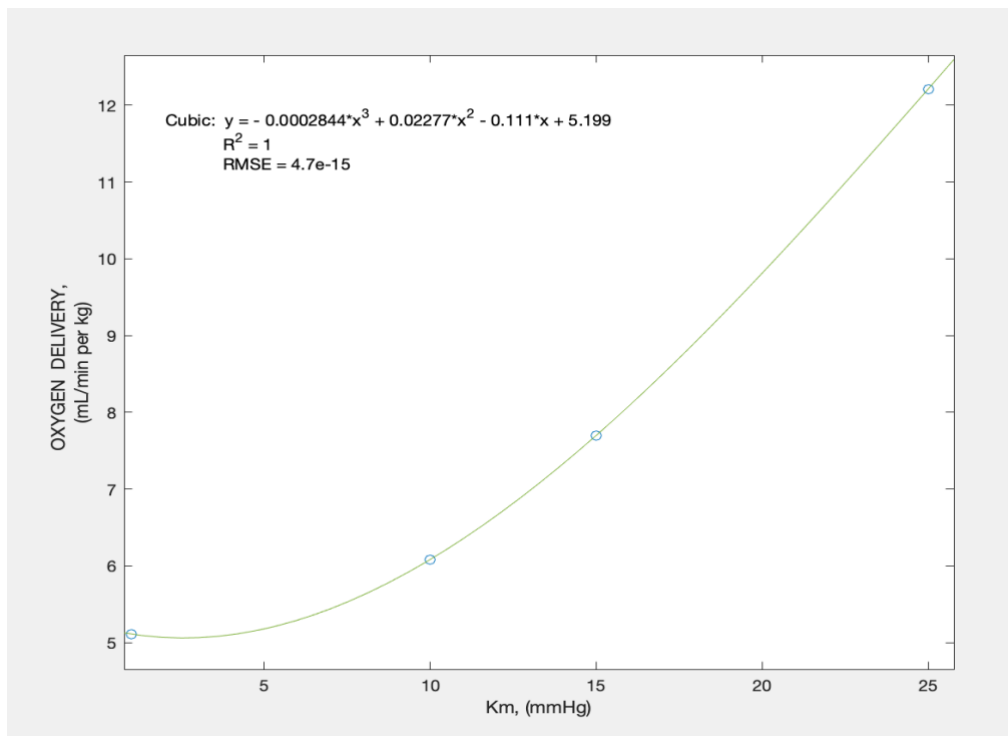
Cubic: $y = -0.0002844 \cdot x^3 + 0.02277 \cdot x^2 - 0.111 \cdot x + 5.199$
$R^2 = 1$
RMSE = 4.7e-15

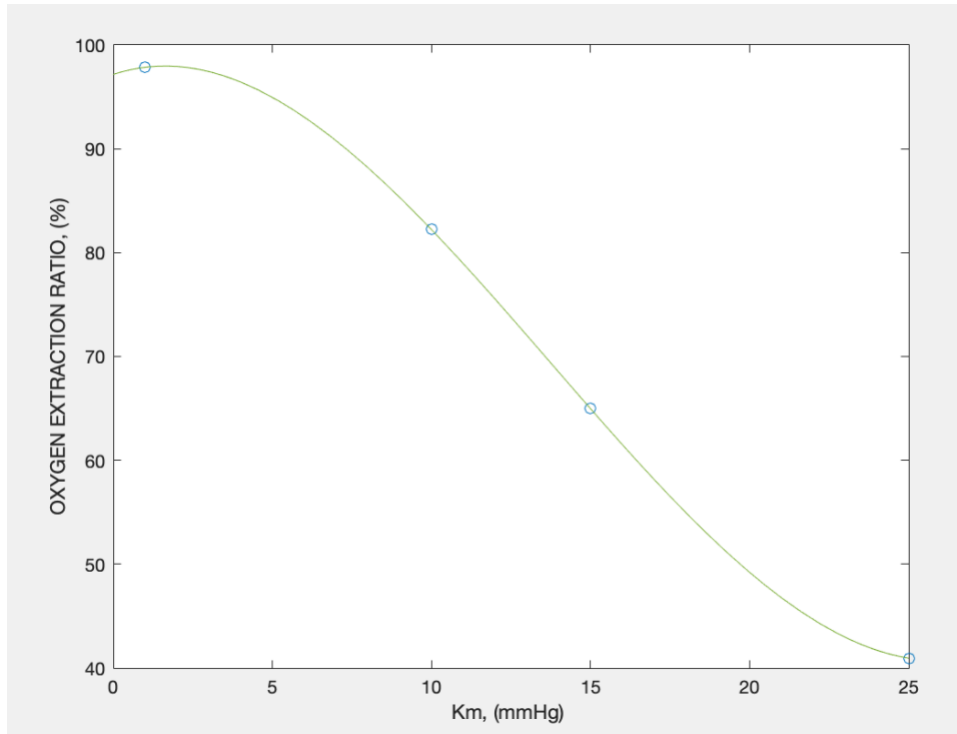Figure 6. The critical points of oxygen delivery and k_m.

Figure 7. The oxygen extraction ratio at the critical oxygen delivery points versus k_m.

The predicted variation of tissue and blood oxygen tension with position in the capillary are shown in Figs. 8-11. The plots were generated for the Schumacker and Samsel model at three different oxygen delivery values of normal, critical, and very low. To compare these curves with Michaelis-Menten oxygen consumption kinetics, the same plots were generated for three values of k_m = 10, 15 and 25 mmHg at three different oxygen delivery values of normal, critical, and a very low value. Figures 8-11 show a decline in tissue and blood oxygen tension along the length of the capillary. Similar declines were observed in all models. The higher the critical oxygen delivery, the lower are the tissue and blood oxygen tension at the end of the capillary.
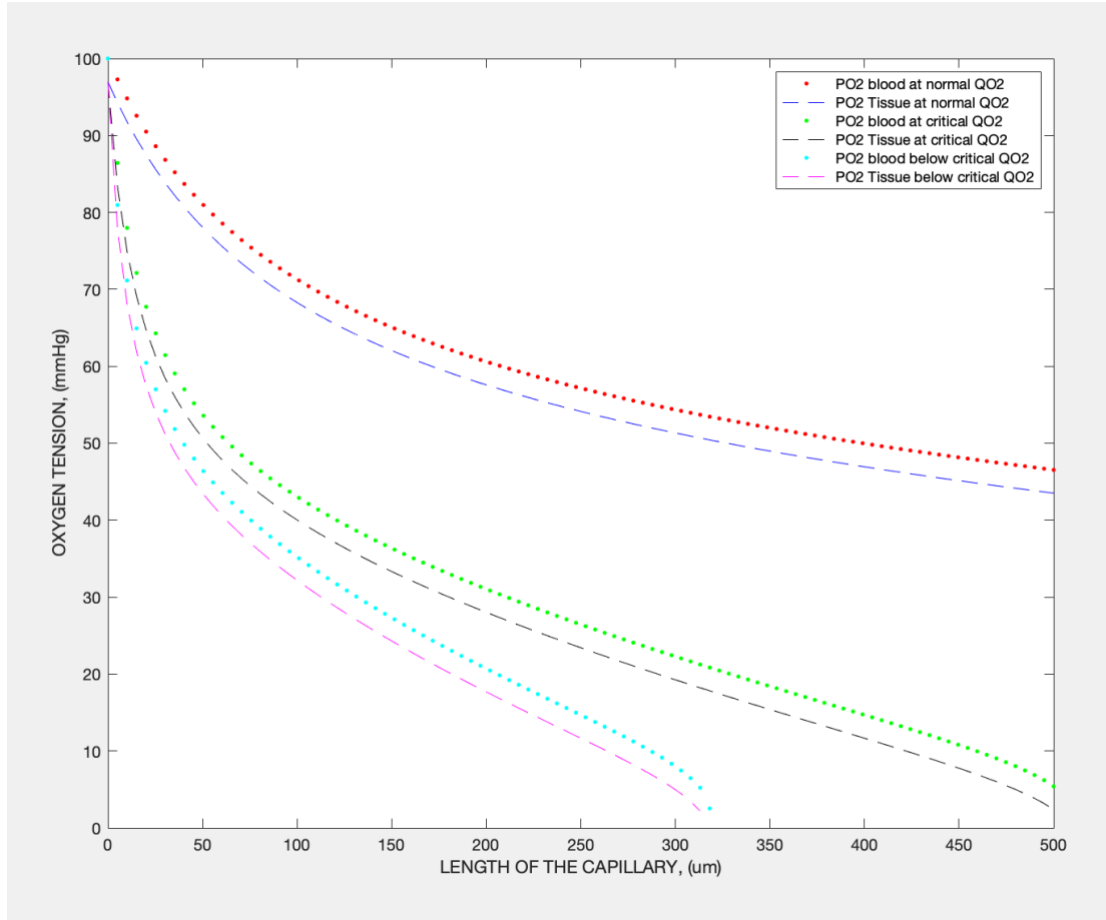
Figure 8. Oxygen tension along the capillary, Schumacker model. Oxygen tension of blood and tissue cylinder are plotted as pairs of curves. Three different pairs of curves (PO$_2$ Blood, PO$_2$ Tissue), respectively, are plotted at normal oxygen delivery (red, blue), critical oxygen delivery (green, black), below critical oxygen delivery (cyan, magenta). Normal oxygen delivery is at cardiac output of 5000 ml/min; critical oxygen delivery is at cardiac output 800 ml/min; low oxygen delivery is at cardiac output 500 ml/min.

Figure 9. Oxygen tension along the capillary, using Michaelis-Menten oxygen consumption kinetics model, where $k_m = 10$ mmHg. Oxygen tension of blood and tissue cylinder are plotted as pairs of curves. Three different pairs of curves (PO$_2$ Blood, PO$_2$ Tissue), respectively, are plotted at normal oxygen delivery (red, blue), critical oxygen delivery (green, black), below critical oxygen delivery (cyan, magenta). Normal oxygen delivery is at cardiac output 5000 ml/min; critical oxygen delivery is at cardiac output 950 ml/min; low oxygen delivery is at cardiac output 500 ml/min.
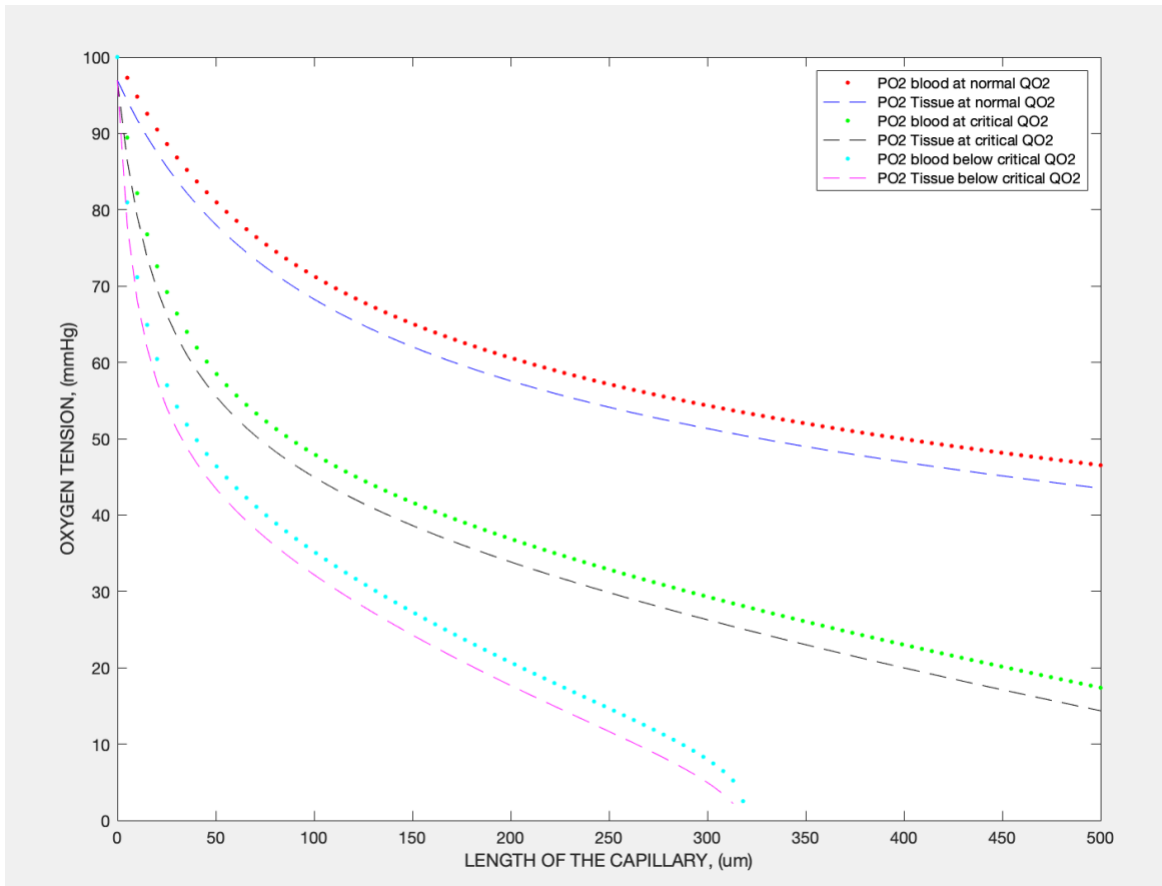
Figure 10. Oxygen tension along the capillary, Michaelis-Menten oxygen consumption kinetics model, where $k_m = 15$ mmHg. Oxygen tension of blood and tissue cylinder are plotted as pairs of curves. Three different pairs of curves (PO$_2$ Blood, PO$_2$ Tissue), respectively, are plotted at normal oxygen delivery (red, blue), critical oxygen delivery (green, black), below critical oxygen delivery (cyan, magenta). Normal oxygen delivery is at cardiac output 5000 ml/min; critical oxygen delivery is at cardiac output 1100 ml/min; low oxygen delivery at cardiac output 500 ml/min.
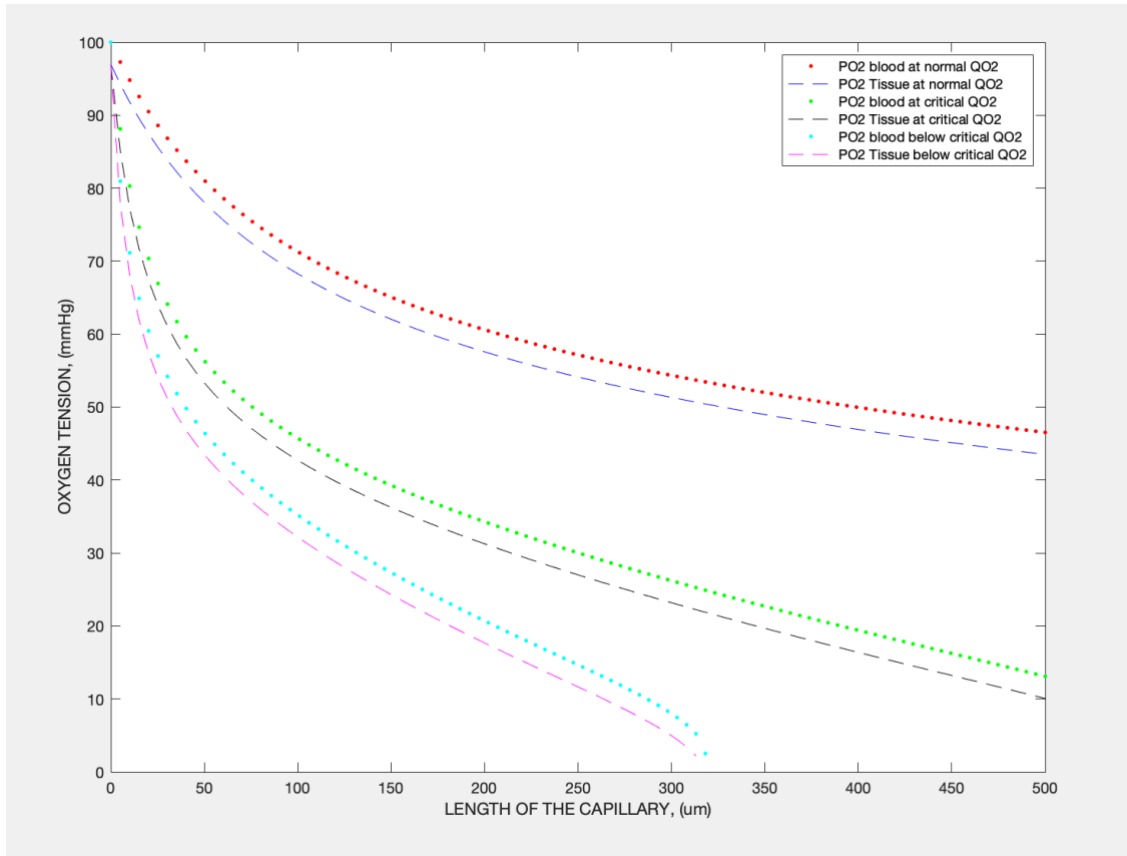
Figure 11. Oxygen tension along the capillary, Michaelis-Menten oxygen consumption kinetics model, where $k_m = 25$ mmHg. Oxygen tension of blood and tissue cylinder are plotted as pairs of curves. Three different pairs of curves (PO$_2$ Blood, PO$_2$ Tissue), respectively, are plotted at normal oxygen delivery (red, blue), critical oxygen delivery (green, black), below critical oxygen delivery (cyan, magenta). Normal oxygen delivery is at cardiac output 5000 ml/min; critical oxygen delivery is at cardiac output 1500 ml/min; low oxygen delivery is at cardiac output 500 ml/min.
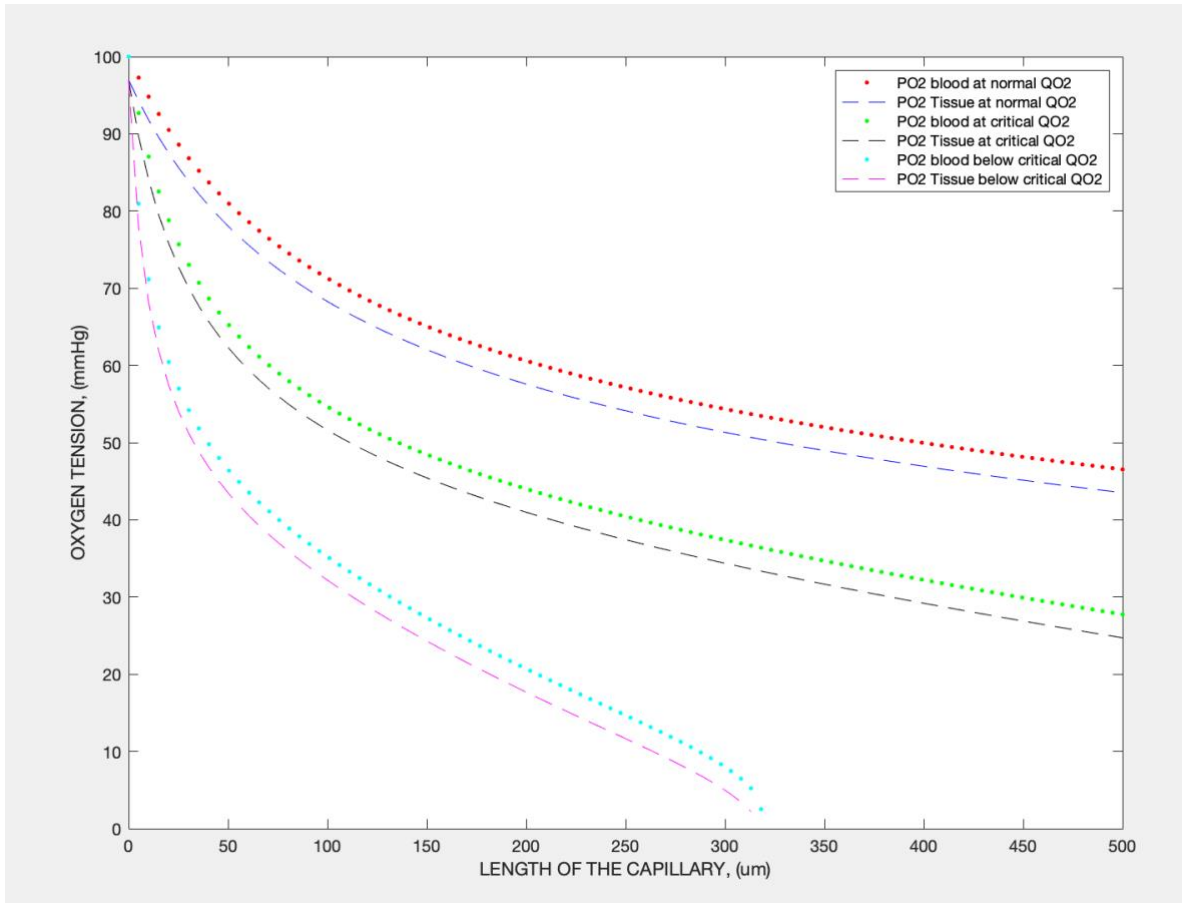
A summary table of critical oxygen delivery, oxygen consumption, oxygen extraction ratio, and venous oxygen tension is reported in Table 3.

	QO_{2crit} (ml/min per kg)	VO_2 (ml/min per kg)	$EO_{2\ crit}$ (%)	PvO_2 (mmHg)
PO_2=1 mmHg	5.11	5.0	97.85	3.98
k_m (mmHg)				
10	6.08	5.0	82.88	11.24
15	7.70	5.0	64.97	15.05
25	12.21	5.0	40.95	25.01

Table 3. Summary of values of critical oxygen delivery, $QO_{2\ crit}$, oxygen consumption at critical oxygen delivery, VO_2, oxygen extraction ratio, $EO_{2\ crit}$, venous oxygen pressure PvO_2, all as a function of k_m. or at $PO_2 = 1mmHg$ (Schumacker).

Discussion

The relationship between the oxygen consumption (VO_2) of an isolated perfused tissue and the rate of delivery of oxygen (QO_2) to the tissue has been a subject of interest to many investigators over the past century. A typical finding has been that there was a critical value of QO_2 below which tissue VO_2 began to decline. Schumacker and Samsel (1989) appear to be the first to attempt a theoretical explanation of this relationship based upon the Krogh tissue cylinder model and its assumptions. They reported a computational model in which they were able to predict the results of experiments giving the relationship between VO_2 and QO_2. Their model assumed a simple relationship between VO_2 and tissue oxygen tension (PO_2), whereby VO_2 was a constant value, V^{max}, for $PO_2 > 1$ mmHg and was zero for $PO_2 \leq 1$ mmHg. More recently, Golub and Pittman (2012) found that the PO_2 dependence of VO_2 in vivo was more accurately described by a Michaelis-Menten kinetics expression where $k_m \approx 10$ mmHg. The work presented in this thesis extended Schumacker and Samsel's computational model to include the more accurate Michaelis-Menten kinetic description of the PO_2 dependence of VO_2.

The major findings of this project are presented in Table 3. The critical oxygen delivery was found to depend on k_m, increasing nonlinearly as k_m increases. The fractional oxygen extraction at the critical QO_2 varied with k_m, where at a higher k_m, the oxygen extraction (EO_2) was lower. The venous oxygen partial pressure (PvO_2) also varied with k_m. Finally, the radial profile of the tissue oxygen tension at the critical QO_2 depended on k_m. At lower critical oxygen delivery and at lower k_m, the critical radial distance at which tissue oxygen partial pressure was found to be k_m occurred closer to the end of the capillary. Based on these results, it is important to note that the oxygen consumption dependence of oxygen delivery covers a wide range of physiological oxygen tension values, as was suggested in previous studies (Golub & Pittman, 2003)

Oxygen consumption and delivery

Previous in vivo studies have investigated the dependency of tissue oxygen consumption on different factors including blood flow, arterial oxygen tension, oxygen extraction ratio, and oxygen delivery. Schumacker suggested that the decline in tissue oxygen consumption is because the tissue oxygen extraction cannot increase below the critical oxygen delivery in proportion to the reduced delivery (Schumacker, 1987). Some studies have shown that below the critical oxygen delivery, extraction has been reported to increase further (Cain, 1983), while other studies report that the extraction ratio at that threshold is a maximum (Cain, 1983). Schumacker later suggested that tissue oxygen tension becomes hypoxic due to the supply limitation beginning when the critical point of PO_2 is below 1 mmHg (Schumacker, 1989). Similarly, an in vitro study measured oxygen consumption rates in mitochondrial suspensions and showed that cellular respiration would be maintained at either relatively low or high oxygen concentrations as long as the oxygen partial pressure was above the critical level of 1 mmHg (Wilson, 1988). More recently, a study by Golub & Pittman study concluded that VO_2 was PO_2-dependent and approximately followed Michaelis-Menten kinetics with a k_m of 10.5 mmHg (Golub & Pittman, 2012).

Other studies have shown that tissue oxygen consumption depended on blood flow. For instance, Bulkley showed that oxygen consumption is independent of blood flow until the blood flow was below 30 ml/min/100 g (Bulkey, 1985). Hughson's study established that there is a positive correlation between oxygen consumption and blood flow in human forearm muscle, and concluded that oxygen consumption can be limited by the availability of oxygen (Hughson, 1996). More recent findings by Kalliokoski suggested that there is a good correlation in blood flow and oxygen consumption in different muscles during exercise, and that endurance-trained men might exhibit a stronger correlation than untrained men (Kalliokoski, 2004).

Other investigators have studied the dependence of tissue oxygen consumption on oxygen delivery. Woerkens studied the critical oxygen delivery at which oxygen consumption starts to decline due to excessive blood loss during surgery in an anesthetized human. He found that the critical point is 4.9 ml O2/min per kg and explained that a reduction in oxygen delivery by reduced cardiac output is often accompanied by even more decreased blood flow through the microcirculation, whereas during hemodilution blood flow is accelerated, owing to the improved rheologic properties of blood (Woerkens, 1992). In animal studies, a critical oxygen delivery was found to be 10 ml/min per kg in anesthetized dogs during hypoxia (Cain, 1977; Cain &Chapler, 1978). Parolari and his colleague have found a direct linear relationship between oxygen delivery and consumption during cardiopulmonary bypass, and under the studied conditions neither a biphasic relation nor a plateau level were demonstrated in any patient. They found that when oxygen delivery decreased there was a concurrent reduction in oxygen consumption that was entirely dependent on oxygen delivery and was due to an increase in oxygen extraction up to 30%, and thus there was a redistribution of blood flow, and some capillary beds became either under-perfused or not perfused at all. Above the critical oxygen delivery point, there was a progressive increase of oxygen consumption concurrent with the increase of oxygen delivery (Parolari, 1995).

The oxygen consumption dependency on oxygen delivery is shown in Figures 4 and 5. In all four plots, similar behaviors are shown in which, as the oxygen delivery was reduced from 32.23 ml O2/min per kg until just before it reached the critical point, oxygen consumption was calculated to be at its maximum. When the critical QO2 point was reached as oxygen delivery was further reduced and a fraction of the tissue cylinder became hypoxic, a non-linear curve appeared with a higher k_m; as a result, overall tissue oxygen consumption decreased. This can be explained by considering the two radial regions of the tissue cylinder volume (i.e., Regions I and II). were

created and was calculated by Michaelis-Menten oxygen consumption kinetics (Eqs. 16-17). Region I from r = rc to r = r* was the tissue closest to the capillary and was assumed to have a maximum oxygen consumption, V^{max}; it was assumed to be in the P_{O2}-independent region for which $PO_2 > k_m$. Region II from r = r* to r = R corresponded to the outer band of tissue and was assumed to be in the P_{O2}-dependent region for which $0 < P_{O2} < k_m$, and (Eq. 17) showed a non-linear relationship between the integrated local oxygen tension over the cross-sectional area of the tissue cylinder and the oxygen consumption per unit volume over that area. Thus, r = r* corresponded to the interface separating the PO_2-independent from the PO_2-dependent region. As the capillary oxygen tension decreased toward the end of the capillary, the area of the P_{O2}-dependent region became larger, leading to a larger faction of tissue volume with $PO_2 < k_m$. The present results suggest that the value of k_m will has an influence on the relationship between tissue oxygen consumption and oxygen supply as the oxygen delivery is reduced to the critical point. However, with Michaelis-Menten kinetics the meaning of the terms "hypoxia" and "normoxia" is not as clear-cut as in the case where mitochondrial oxygen consumption is viewed as an "on/off" process in regard to a critical mitochondrial PO_2; for the Michaelis-Menten kinetic model, k_m becomes the fundamental parameter that specifies how oxygen consumption depends on oxygen tension instead of the critical mitochondrial oxygen tension.

Oxygen delivery, oxygen extraction ratio, venous oxygen tension and km

Figures 6 and 7 show the predicted relationship between the tissue oxygen tension at different k_m, the critical oxygen delivery, and the oxygen extraction ratio at the critical QO_2. After fitting the data, the graphs show that there is an increasing nonlinear relationship between critical oxygen delivery as k_m increases, while the oxygen extraction ratio at critical QO_2 decreases with increasing k_m. This nonlinear relationship can be explained in part by the nonlinear oxygen dissociation curve relating hemoglobin oxygen saturation and oxygen tension. The arterial oxygen partial pressure is an important part of the oxygen sensing system that responds to changes in the microenvironment. The oxygen saturation is a relative measurement of the concentration of oxygen bound to hemoglobin within the red blood cells. The fractional oxygen extraction is the ratio of the arteriovenous oxygen concentration difference to the arterial oxygen concentration. Oxygen delivery (QO_2) to a region is defined as the rate at which oxygen moves by convection into that region and is the product of blood flow and inflow oxygen content or oxygen concentration (Eq. 9). Neglecting dissolved oxygen in the blood, oxygen concentration or content reversibly bound to hemoglobin depends on hemoglobin oxygen saturation and is related to oxygen partial pressure, as described by the oxygen dissociation curve. The venous oxygen partial pressure was found to be higher when the critical oxygen delivery was higher (which was the case for higher values of k_m), and ranged between 11.2 and 25.0 mmHg. The earlier along the capillary that this k_m is reached, the critical oxygen delivery is reached, and the greater the fractional volume of tissue that becomes hypoxic and the greater the percent fall in oxygen consumption from normal.

Oxygen tension profiles

The oxygen tension profiles along the capillary for the different values of k_m are shown in Figs 8-11. The behavior of the Krogh model in regard to axial or longitudinal tissue and capillary PO_2 profiles were as expected, where both the blood and tissue oxygen tension decrease along the capillary. Generally, for the four different values of k_m normal oxygen delivery shows a lower reduction in oxygen tension than at the critical point and at very low or insufficient delivery. The main difference between all four curves was that the blood and tissue oxygen tension at the critical oxygen delivery shows different behavior. At lower k_m, the blood and tissue oxygen tension profiles along the capillary were reduced greatly compared to normal oxygen delivery. At higher k_m, the blood and tissue oxygen tension profiles along the capillary were close to the behavior of normal oxygen delivery and less reduction in the blood and tissue oxygen tension.

References

Andersen, P., & Saltin, B. (1985). Maximal perfusion of skeletal muscle in man. The Journal of Physiology, 366(1), 233–249.

Blomstrand, E., Rådegran, G., & Saltin, B. (1997). Maximum rate of oxygen uptake by human skeletal muscle in relation to maximal activities of enzymes in the Krebs cycle. The Journal of Physiology, 501(Pt 2), 455–460.

Bulkley, G. B., Kvietys, P. R., Parks, D. A., Perry, M. A., & Granger, D. N. (1985). Relationship of blood flow and oxygen consumption to ischemic injury in the canine small intestine. *Gastroenterology*, *89*(4), 852–857.

Cain SM (1983) Peripheral oxygen uptake and delivery in health and disease. Clin Chest Med 4:139 5.

Cain SM, Bradley WE (1983) Critical O2 transport values at lowered body temperatures in rats. J Appl Physiol 55:1713

Cain, S. M. (1977). Oxygen delivery and uptake in dogs during anemic and hypoxic hypoxia. Journal of Applied Physiology, 42(2), 228–234.

Cain, S. M., & Chapler, C. K. (1978). O2 extraction by hind limb versus whole dog during anemic hypoxia. Journal of Applied Physiology, 45(6), 966–970.

Constanzo, L. S. (1998). Physiology. Philadelphia, W.B. Saunders company.

Eichacker, P. Q., Banks, S. M., Ailing, D. W., Hoffman, W. D., Mouginis, T., Richmond, S., MacVittie, T. J., & Natanson, C. (1990). The relationship of oxygen consumption to oxygen delivery differs in anesthetized vs conscious dogs. Critical care medicine, 18 (supplement), s183.

Golub, A. S., & Pittman, R. N. (2012). Oxygen dependence of respiration in rat spinotrapezius muscle in situ. AJP: Heart and Circulatory Physiology,303(1). doi:10.1152/ajpheart.00131.2012

Hughson, R. L., Shoemaker, J. K., Tschakovsky, M. E., & Kowalchuk, J. M. (1996). Dependence of muscle VO2 on blood flow dynamics at onset of forearm exercise. *Journal of applied physiology (Bethesda, Md. : 1985)*, *81*(4), 1619–1626.

Kalliokoski, K. K., Knuuti, J., & Nuutila, P. (2005). Relationship between muscle blood flow and oxygen uptake during exercise in endurance-trained and untrained men. Journal of Applied Physiology, 98(1), 380–383.

Kelman, G. R. (1966). Digital computer subroutine for the conversion of oxygen tension into saturation. Journal of applied physiology (1948), 21(4), 1375–1376.

Krogh, A. (1919). The number and distribution of capillaries in muscles with calculations of the oxygen pressure head necessary for supplying the tissue. *The journal of physiology*, *52*(6), 409–415.

Parolari, A., Alamanni, F., Gherli, T., Bertera, A., Dainese, L., Costa, C., Schena, M., Sisillo, E., Spirito, R., Porqueddu, M., Rona, P., & Biglioli, P. (1999). Cardiopulmonary bypass and oxygen consumption: oxygen delivery and hemodynamics. The Annals of Thoracic Surgery, 67(5), 1320–1327.

Pishchany, G, Skaar E. P. Taste for blood: hemoglobin as a nutrient source for pathogens. Heitman J., ed. Plos pathogens. 2012;8(3):e1002535.

Pittman, R. N. (2011). Regulation of tissue oxygenation. Morgan & Claypool.

Richardson, R. S., Knight, D. R., Poole, D. C., Kurdak, S. S., Hogan, M. C., Grassi, B., & Wagner, P. D. (1995). Determinants of maximal exercise VO2 during single leg knee-extensor exercise in humans. American Journal of Physiology. Heart and Circulatory Physiology, 268(4), H1453–H1461.

Richardson, R. S., Poole, D. C., Knight, D. R., Kurdak, S. S., Hogan, M. C., Grassi, B., Johnson, E. C., Kendrick, K. F., Erickson, B. K., & Wagner, P. D. (1993). High muscle blood flow in man: is maximal O2 extraction compromised? Journal of Applied Physiology, 75(4), 1911–1916.

Rowell, L. B., Saltin, B., Kiens, B., & Christensen, N. J. (1986). Is peak quadriceps blood flow in humans even higher during exercise with hypoxemia. American Journal of Physiology. Heart and Circulatory Physiology, 251(5), H1038–H1044.

Samsel, R. W., & Schumacker, P. T. (1988). Determination of the critical O2 delivery from experimental data: sensitivity to error. Journal of applied physiology, 64(5), 2074–2082.

Schumacker, P. T., & Cain, S. M. (1987). The concept of a critical oxygen delivery. Intensive Care Medicine, 13(4), 223–229.

Schumacker, P. T., & Samsel, R. W. (1989). Analysis of oxygen delivery and uptake relationships in the Krogh tissue model. Journal of Applied Physiology, 67(3), 1234–1244.

Schumacker, P. T., Long, G. R., & Wood, L. D. (1987). Tissue oxygen extraction during

hypovolemia: role of hemoglobin p50. Journal of Applied Physiology, 62(5), 1801–1807.

Schumacker, P. T., Rowland, J., Saltz, S., Nelson, D. P., & Wood, L. D. H. (1987). Effects of hyperthermia and hypothermia on oxygen extraction by tissues during hypovolemia. Journal of Applied Physiology (1985), 63(3), 1246–1252.

Shibutani, K., Komatsu, T., Kubal, K., Sanchala, V., Kumar, V., & Bizzarri, D. V. (1983). Critical level of oxygen delivery in anesthetized man. Critical Care Medicine, 11(8), 640–643.

Van Woerkens, E. , Trouwborst, A. , van Lanschot, J. & (1992). Profound Hemodilution. *Anesthesia & Analgesia, 75* (5), 818-821.

Wilson, D.F., Erecinska, M. Effect of oxygen concentration on cellular metabolism. Chest 88: 229S-232S, 1985

Wilson, D. F., Rumsey, W. L., Green, T. J., & Vanderkooi, J. (1988). The oxygen dependence of mitochondrial oxidative phosphorylation measured by a new optical method for measuring oxygen concentration. Journal of Biological Chemistry, 263(6), 2712-2718.

Vita

Raghad Abdullah Alqahtani was born on March 02, 1995, in Riyadh, Saudi Arabia. She graduated from Jarir Private High School in June 2013. She received her Bachelor of Science in Biomedical Engineering from Virginia Commonwealth University in May 2019 and went on to receive a Master of Science in Physiology and Biophysics from Virginia Commonwealth University in August, 2021.